Characteristics of GDI Engine Flow Structures

Merkmale der Strömungsstrukturen eines Benzinmotors mit Direkteinspritzung

Mr N. J. Beavis,
Department of Aeronautical and Automotive Engineering, Loughborough University, Loughborough, UK

Dr S. S. Ibrahim,
Department of Aeronautical and Automotive Engineering, Loughborough University, Loughborough, UK

Dr. P. K. Manickam,
Department of Aeronautical and Automotive Engineering, Loughborough University, Loughborough, UK

Prof. W. Malalasekera,
Department of Mechanical Engineering, Loughborough University, Loughborough, UK

To cite this article: N.J. Beavis et al., Characteristics of GDI Engine Flow Structures, in Engine Combustion Processes (Alfred Leipertz, Editor), ESYTEC GmbH, Erlangen 2015, pp. 385-396.

The benefits of the gasoline direct injection engine over the more traditional gasoline port-fuel injection engine are well known and include the ability to operate lean of stoichiometric for fuel efficiency improvements, reduced knock propensity and reduced unburned hydrocarbons during cold start and transients. Nevertheless, a number of key challenges still remain including cyclic variability, abnormal combustion phenomena and increased particulate emissions. Our progress in each of these challenges is intrinsically linked to our understanding of the flow field formed within the cylinder.

This paper presents the development, validation and subsequent utilisation of a 3D-CFD gasoline direct injection engine model for making predictions of the in-cylinder flow field through the intake and compression strokes.

An extensive validation exercise was completed using experimental data from a single cylinder optical research engine to validate both the intake runner, intake valve jet and in-cylinder flow fields. Validation results showed the model to generally compare well against experimental data including indicating data, intake runner velocities and flow momentum, valve jet and in-cylinder flow structures. Differences were identified in the timing of the detachment of the intake valve jet from the cylinder head and a subsequent reduction in effective flow area was hypothesised as contributing to an over prediction of the valve jet and in-cylinder flow velocities. A comparison of the spatial and temporal development of the in-cylinder flow field identified the model to well predict the flow structures through the intake and compression stroke.

The model was then exercised with a view to evaluate the impact of solid boundaries on the spatial and temporal development of the in-cylinder flow structure. An analysis on the impact of using a pent-roof optical access window in research engines on the flow structure is also provided, indicating that significant asymmetry and additional

recirculation zones in the corners of the access window should be considered when evaluating experimental results from a research engine of this configuration.

1. Introduction

The benefits of the gasoline direct injection (GDI) engine over the more traditional port-injection strategy are well known and include:

- Eliminated transient dwell time associated with the time taken for fuel to be inducted into the cylinder
- Reduced unburned hydrocarbons during cold start and transient excursions
- Reduced knock propensity due to charge cooling effects. Improved fuel efficiency due to improvements in the accuracy of fuel metering and the ability to operate across a number of fuel injection strategies

Even with these improvements, the GDI engine still holds a number of research challenges. Cycle-to-cycle variability in SI engines has long been a topic of research interest. A literature survey was completed on cyclic variability in spark ignition engines and the findings suggested that up to a 10% improvement in fuel consumption would be achievable if it was possible to eliminate cyclic variability entirely [1]. Abnormal combustion phenomenon including engine knock and methods to mitigate it, have been a long standing challenge to engine development. The temperature and pressure histories of the end gas are governed by the propagating turbulent flame front which in turn is directly affected by the in-cylinder flow field. GDI engines also suffer from higher particulate matter emissions and the characterisation and investigation into mitigation methods have been of significant interest to both academia and industry since the introduction of both particle number and particle mass legislation EU6b in 2014. An ability to study and understand the in-cylinder flow field and its impact on the fuel injection, mixing and combustion processes is a key input in support of these research challenges.

2. Experimental Engine Description

The experimental data used to validate the computational results was taken from a single cylinder four stroke motored optical research engine designed and built by the advanced powertrains group of Jaguar Cars. The engine design was based on the combustion chamber of a V8 engine with pent-roof cylinder head and four valves per cylinder. The engine features a ‘Bowditch’ piston arrangement and fused silica piston crown, cylinder liner and pent-roof window to allow significant optical access to the combustion chamber. The engine also features a clear resin intake runner for optical access to the intake runner flow field. The flow field was imaged using a Time Resolved Digital Particle Image Velocimetry (TRDPIV) system including double pulse laser and high speed camera. The experimental setup is described in detail in publications [2,3].

3. Engine Model Description

An engine model was developed using the CFD code STAR-CD (ver 4.20) for the purpose of modelling the in-cylinder flow field through intake and compression strokes.

3.1 Computational Domain

The computational domain is illustrated in Figure 1.

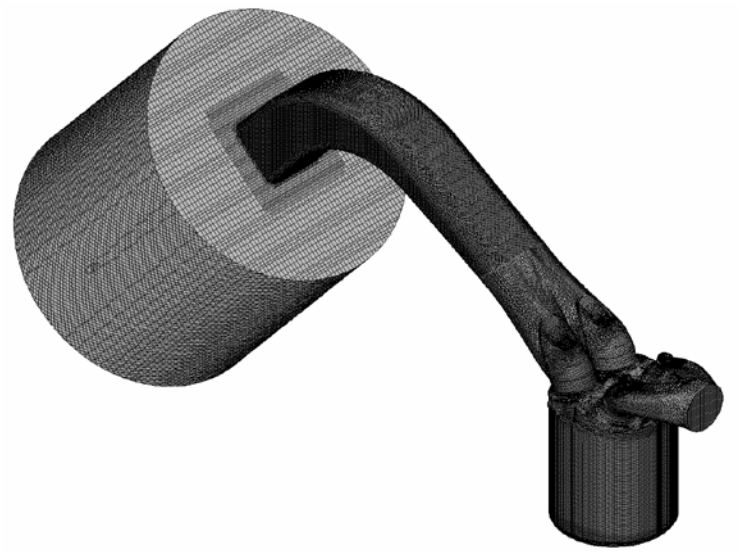

Figure 1 - The computational domain and mesh developed as a representation of the experimental configuration

A grid dependency study was completed prior to model validation. Six different meshes were evaluated, ranging from 1.25million cells to 2.6million cells at BDC. Both qualitative and quantitative results (not shown here) suggested that a mesh size of approximately 2.2million cells at BDC was required to establish a solution that was mesh size independent. Final cell size in the cylinder interior was approximately $1mm^3$.

A fireland was added to represent the crevice volume between the piston crown and the top ring of the ring pack. This volume is typically more substantial with optical research engines due to the need to use specialist materials with increased clearance gaps to protect the optical cylinder liner. The large surface-to-volume ratio of this volume subsequently yields high heat transfer rates hence its inclusion allows the model to better match the experimental cylinder volume and overall heat transfer rates.

3.2 Boundary and Initial Conditions

The inflow at the intake plenum is specified as a constant-pressure constant-temperature environment in the absence of time varying experimental data. The inflow pressure was reduced by 7% from the experimental intake pressure to better match the in-cylinder intake stroke pressure-volume profile. This was considered a reasonable adjustment based on an uncertainty of the experimental measurement location and uncertainty associated with the measurement system itself.

The outflow at the exhaust port-manifold interface was also specified as a constant-pressure constant-temperature boundary condition. In this instance, the pressure distribution profile from the domain interior is applied where the mean of this profile is equal to the supplied outflow pressure.

The intake and exhaust valve lift profiles were derived from the predicted cam profiles with further adjustments made based on experimental data for variation in lift due to thermal expansion of the cylinder head and valve and lash settings.

An initial condition sensitivity study was carried out where four complete engine cycles were simulated with each successive cycle being initialised using the results from the previous cycle. The results (not shown here) showed that a minimum of two cycles were

needed to establish an initial condition independent solution, primarily to establish the correct prediction of intake system wave dynamics and their subsequent impact on the in-cylinder flow field.

3.3 Turbulence Modelling

The RANS approach was used for the modelling of turbulence. The Renomalization Group (RNG) k-ε turbulence model was used [4,5] as an alternative to the standard k-ε model due to reports of it more effectively accounting for the effects of compression, expansion and rapid strain on the turbulence scales found inside the cylinder through an additional term in the energy dissipation ε-equation representing the effect of mean flow distortion on turbulence [6]. The formulation of the RNG k-ε model used also accounts (to some extent) for compressibility and buoyancy effects.

4. Results and Discussion

4.1 Model Validation

The model is validated against published experimental data at a standardised motored condition as depicted in Table 1, with the exception of the intake system validation which was performed at an intake manifold pressure of 700mbar due to experimental data availability.

Engine Speed	1500 rpm
Barometric Pressure	1007 mbar
Intake Manifold Pressure (gauge)	528 mbar
Intake Temperature	28 °C
Exhaust Backpressure (gauge)	16 mbar
Exhaust Temperature	511 °C

Table 1 - Experimental motoring condition used for model validation

Before beginning an in-depth evaluation of the predicted flow field, the model was first compared against experimental indicating data. Figure 2 shows the pressure-volume history on a log-log scale and shows the model to be in good agreement with experimental data. The close match around IVC and EVO provides confidence in the adjustments made to the valve lift profiles to account for lash and thermal expansion.

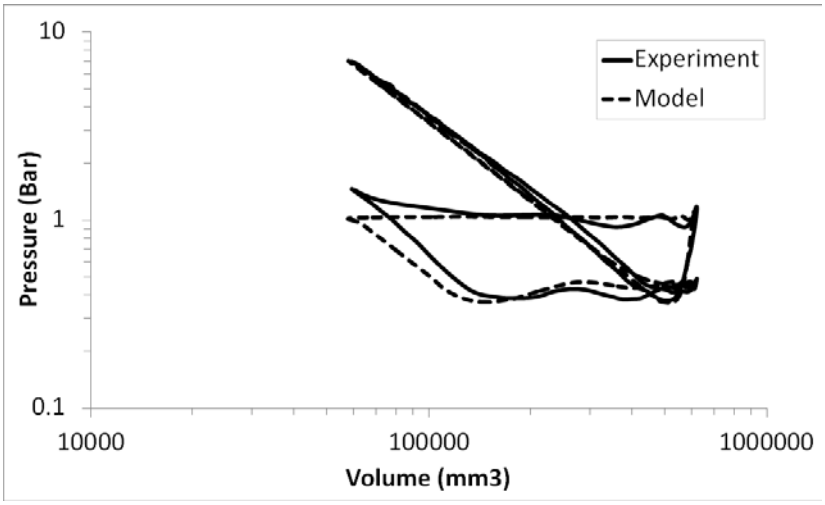

Figure 2 – A comparison of experimental and CFD model predictions for in-cylinder pressure-volume data on a log-log scale

Next the model was validated with respect to its ability to predict the conditions within the intake runner. The predicted intake runner velocity is compared against the available experimental velocity data at discrete crank angles as shown in Figure 3. Following this, the experimental intake runner momentum was compared against model intake valve curtain flux, as shown in Figure 4. Whilst these two data sets are not directly comparable, a qualitative comparison provides useful insight into how accurately the model is predicting changes in flow momentum as a consequence of wave dynamics. Figure 3 and Figure 4 both indicate that the model is well suited to predict the intake system flow field. Experimental data sets in Figure 3 and Figure 4 are taken from [2] where a complete description of the experimental setup and post-processing techniques used are given.

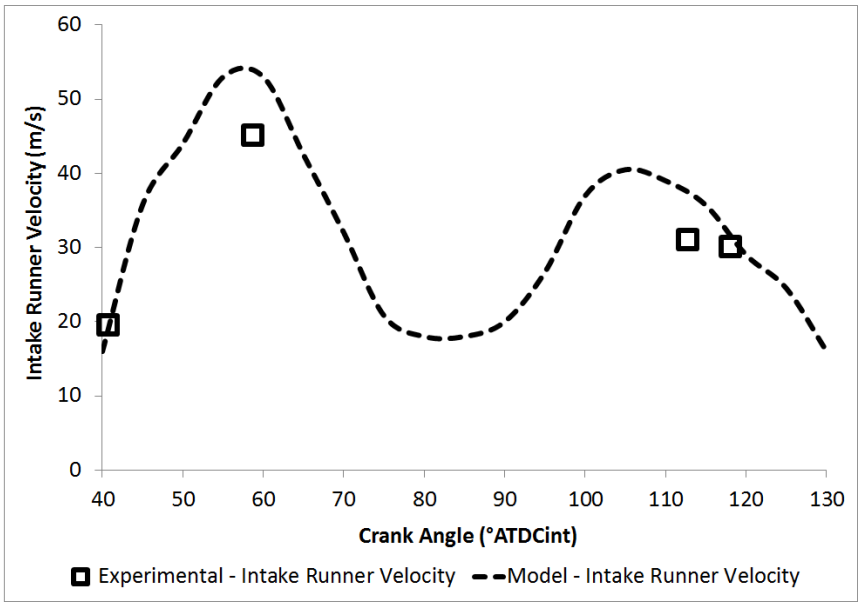

Figure 3 – A comparison of experimental and CFD model predictions for intake runner velocity, experimental data taken from [2]

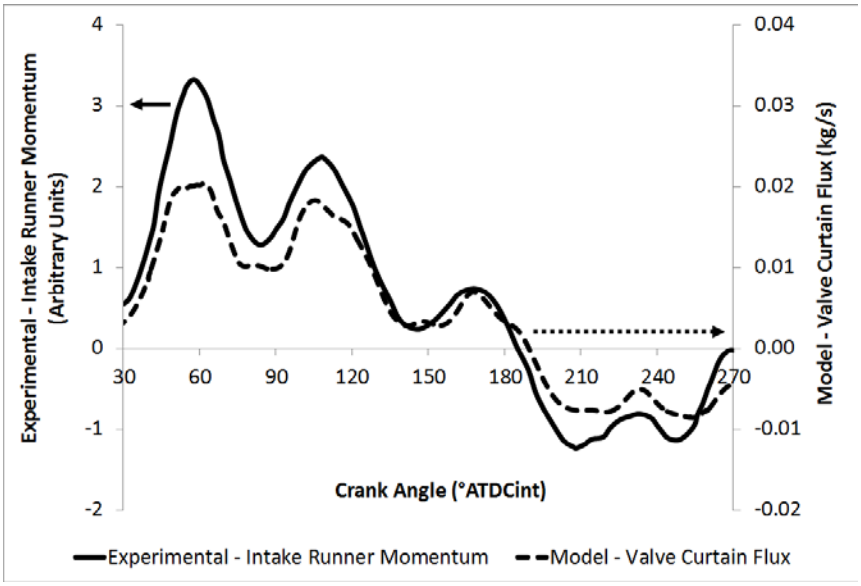

Figure 4 – A comparison of experimental intake runner momentum taken from [2] *and CFD model predictions of valve curtain flux*

Experimental PIV data in the pent roof region focussed on the intake valve jet and was used to validate the model flow field predictions for flow entering the cylinder past the intake valve. Experimental data from [7,8] was used, where the experimental set-up and data capture method is described in detail. Due to the large degree of cyclic variability seen in this flow structure, the experimental PIV data used to support model validation is a combination of both the mean low frequency flow fields and raw flow field data. Whilst the mean low frequency flow fields offer a more direct comparison to a RANS model prediction, the raw flow fields also provided details on some of the cycle-to-cycle variations in the flow field and offer the potential for providing insight into differences between predictions and experiments.

Figure 5 shows a comparison between the mean low frequency flow field from experimental data and the predicted flow field for the intake valve jet. The figures show that the flow field structure is well predicted with respect to the positioning of recirculation zones and valve jet angle. The velocity profile is reasonably well predicted over the crank angles shown with a slight over prediction of valve jet velocity later in the cycle as shown by the images at 100°ATDC$_{int}$.

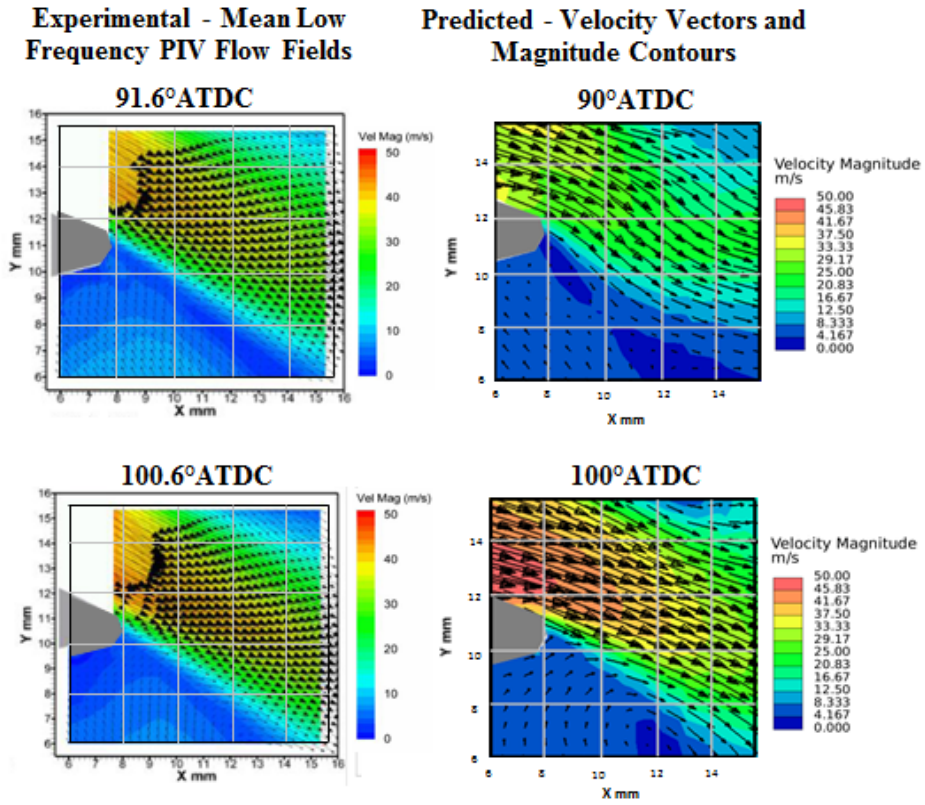

Figure 5 - A comparison of mean low frequency PIV flow fields [7] *and CFD model predicted flow fields for the intake valve jet*

Figure 6 provides a comparison of the model predictions against experimental PIV data from a single cycle. Here it can be seen that the intake valve jet is predicted to detach from the cylinder head at a lower valve lift than seen in the experimental data. This will drive differences between the predicted discharge coefficient and that of experiments. It is well known that the valve discharge coefficient is intrinsically linked to the flow field past the valve and hence changes in flow field as a consequence of flow detaching from

a particular surface causes a subsequent change in discharge coefficient. In this case, the model predicts the valve jet to detach from the cylinder head at lower valve lift thus it could be theorised that this will act to lower the discharge coefficient, reduce the effective flow area and cause a subsequent over prediction of valve jet velocity. Unfortunately experimental data is not available to validate this hypothesis.

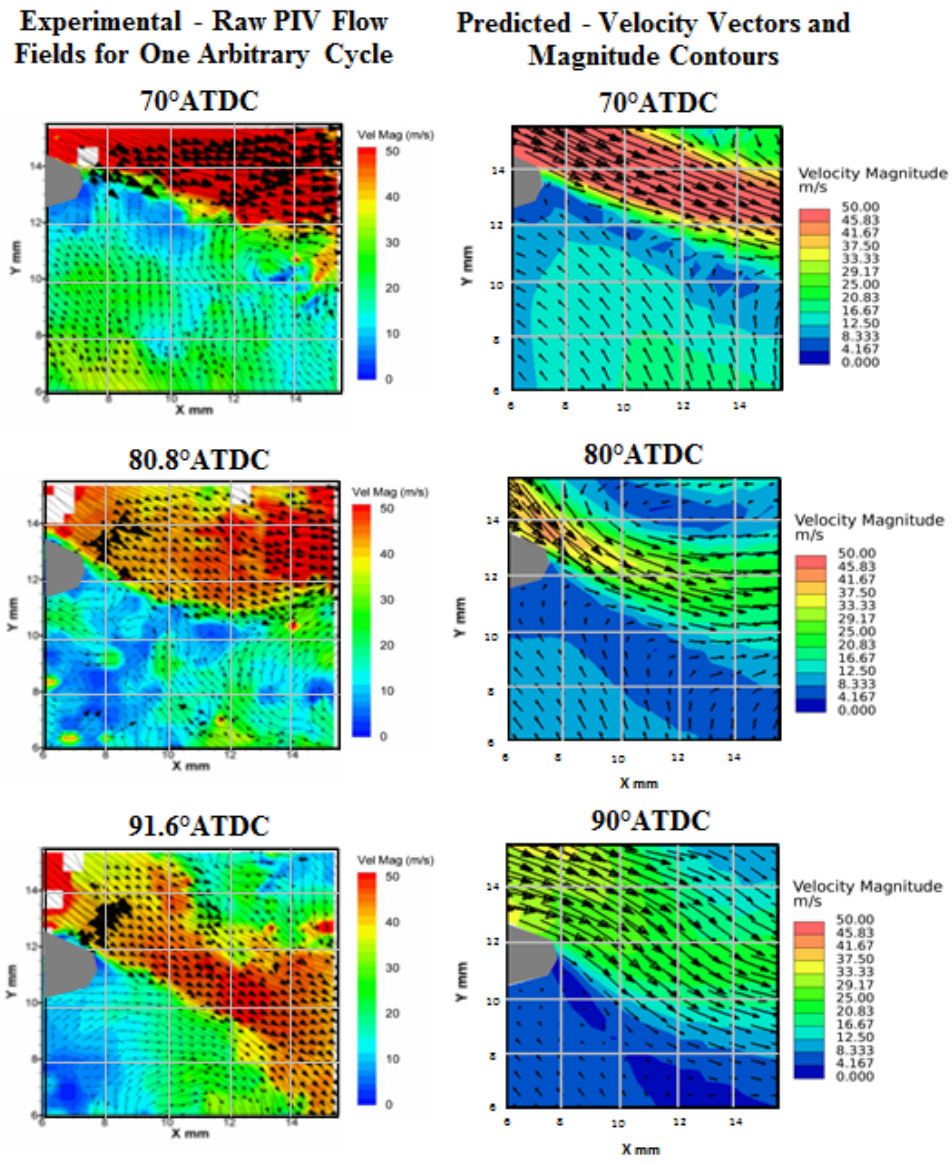

Figure 6 – A comparison of raw PIV flow fields for one arbitrary cycle [8] *and CFD model predicted flow fields for the intake valve jet*

Additional experimental data was reviewed [8] (not shown here) for a number of engine cycles at 70°ATDC$_{int}$ and 97°ATDC$_{int}$. The data illustrates the difficulty of validating a CFD model using time-averaged turbulence modelling for highly unstable flow fields with strong shear flows that are present in the intake valve jet. The data indicates that a high degree of cyclic variability is present early in the intake valve jet development period with some cycles showing the valve jet still attached to the cylinder head whereas other cycles show varying levels of detachment. By 97°ATDC$_{int}$ the data shows that the valve jet exhibits significantly less cycle-by-cycle variation in flow structure indicating that the valve jet is more stable by this point in the cycle.

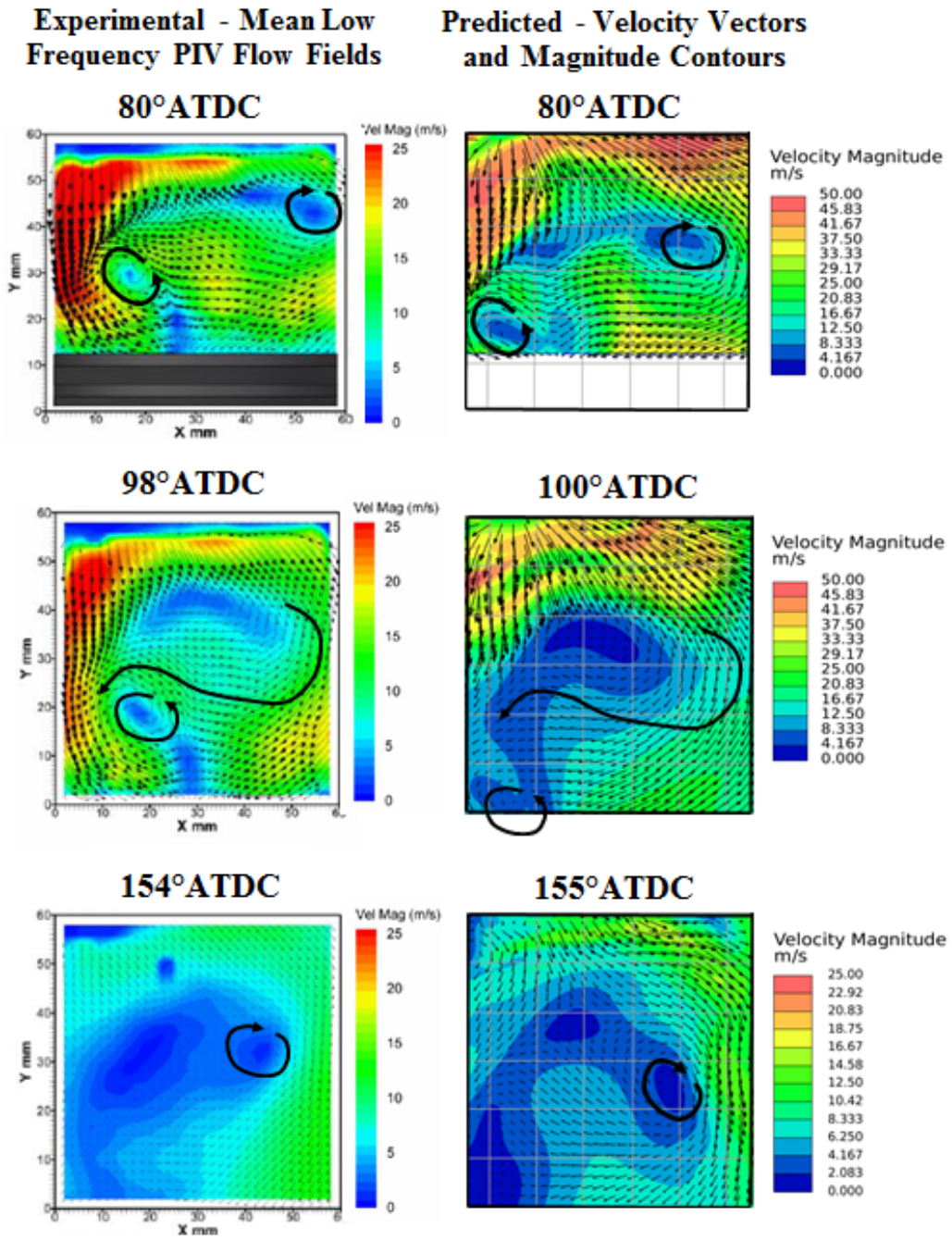

Figure 7 – Experimental PIV data [7] *compared against CFD model predicted flow fields along the bore centre line in the tumble plane, with black arrows indicating similarities in flow structures between experiment and model*

The in-cylinder flow field was validated using experimental PIV data [7] along the bore centreline in the tumble plane and comparative figures are presented in Figure 7. The engine presented here has a fairly weak tumble ratio due to the intake port and valve geometry and as a consequence, the flow structures generated by the flow past the intake valve and subsequent interactions with cylinder walls are also weaker in comparison to an engine with a strong tumble ratio. Weaker flow structures are inherently more challenging to model due to being more susceptible to the influence of cyclic variations in turbulence. This particular engine was also configured to exhibit

higher than normal levels of cyclic variation which also makes predicting the in-cylinder flow structure difficult with a Reynolds averaged turbulence model.

It is clear from Figure 7 that at 80° and 100°ATDC$_{int}$, the in-cylinder velocities are over predicted by the model when compared against the PIV data presented here (note the difference in contour scales). As discussed previously, this is thought to be due to the over prediction of intake valve jet flow. This is of particular note when modelling a homogeneous GDI engine where injection is early in the intake process, since the over predicted in-cylinder flow velocities have the potential to more strongly influence the fuel spray break-up and atomisation processes and mixture cloud distribution than would be seen in experiment. That said, in general the flow structures are fairly well predicted by the model. There are clear similarities in predicted and measured recirculation regions, though the exact positioning within the cylinder is sometimes not perfectly predicted. The model provides a good basis for understanding the in-cylinder flow structures occurring within a single cylinder optical GDI research engine and for making deductions on the impact of the spatial and temporal development of the flow structure on other in-cylinder processes including injection, combustion and pollutant formation.

4.2 In-Cylinder Flow Structures based on CFD Results

As discussed above, this engine exhibits a relatively weak tumble flow structure (tumble ratio of approximately 0.5) which is evident from the similar magnitude velocity valve jets forming either side of the intake valve due to the relatively straight intake port geometry and shallow pent-roof. This is clearly visible from the image at 70°ATDC Figure 8 (a). The lack of separation of the intake valve jet from the valve seat is also indicative of this observation. Due to valve jets being formed on both sides of the intake valve and the obvious axis asymmetry due to the intake valve being positioned on one side of the cylinder, a number of complex flow structures are generated through the intake and compression strokes.

An interesting turbulent flow structure is generated on the nearside cylinder wall at 70°ATDC$_{int}$ as a consequence of the strong intake valve jet and flow interacting with the piston which is still relatively high in the combustion chamber illustrated by black annotations in Figure 8 (a). By 85°ATDC$_{int}$ the flow structure is largely dissipated due to the falling piston and weakening valve jet but injection timings prior to this could lead to fuel being trapped in this recirculation zone and be the source of fuel absorption into the liner oil film.

The reduced impact of the piston crown on in-cylinder flow structures later in the intake stroke is highlighted by Figure 8 (b) and (c). It is evident that earlier in the cycle the flow field is heavily influenced by tumble flow rebounding off the piston crown. By 110°ATDC$_{int}$ the piston is significantly lower in the cylinder, which reduces the likelihood of rebounding flow structures interacting with flow structures in the centre and upper portions of the combustion chamber. This allows much more symmetrical recirculation regions to form underneath the intake valves.

Another appropriate use of this model is to study the impact of the pent-roof optical access window on in-cylinder flow structures. This is of particular interest to experimentalists looking to compare experimental results from an engine with pent-roof access window against results from a thermal engine.

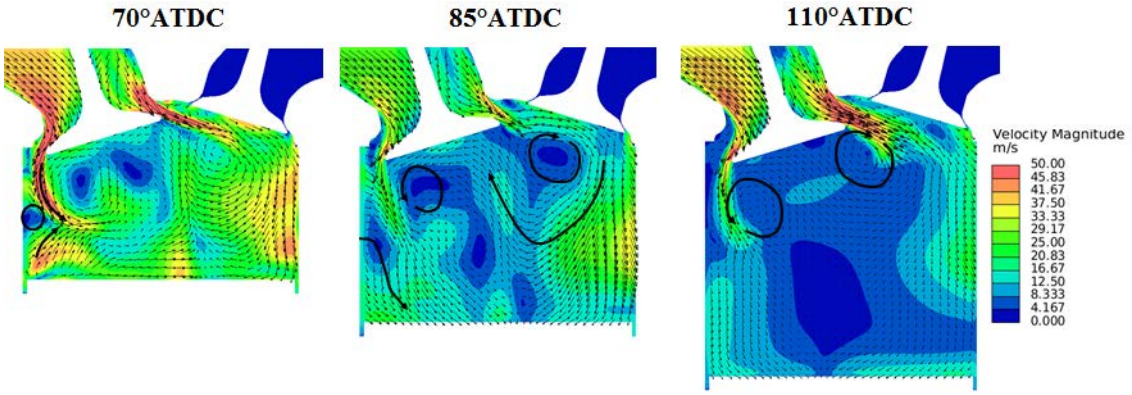

(a) (b) (c)

Figure 8 – CFD model predicted flow fields at 70°, 85°and 110°ATDC, illustrating a recirculation zone close to the cylinder wall and the impact of solid boundaries on in-cylinder flow structures at different points in the intake stroke

The Figure 9 (a) shows velocity vectors and magnitude contours along a swirl cutting plane intersecting the optical access window. The presence of two additional turbulent eddies on the front side of the cylinder are evident as a consequence of the abrupt geometry of the optical access window. This has the effect of generating significant front-to-rear flow asymmetry.

The Figure 9 (b) is along the head gasket swirl plane and again illustrates the flow asymmetry generated by the optical access window. It is clear that the flow field from the rear of the combustion chamber is stronger due to the rounded cylinder wall. The intersection of flow fields from the front and rear of the combustion chamber also occurs in a different plane generating additional recirculation regions, highlighted by the black arrows on the figure. Both Figure 9 (a) and (b) also identify the sharp corners of the optical access window generating recirculation regions that are not present at the rear of the combustion chamber.

From these predictions, a number of considerations can be proposed for experimentalists using a pent-roof access window.

- As a consequence of flow asymmetry:
  - The flow field is less representative of the flow field generated in an engine without the pent-roof window
  - The choice of experimental measurement location is of greater significance
  - Predictions suggest that the influence of the optical access window on the in-cylinder flow field is largely limited to the pent-roof region
  - There will be an impact on fuel spray symmetry and final flow structure in the near spark plug region at the point of ignition timing
- As a consequence of additional recirculation zones in the pent-roof window:
  - An opportunity for mixture non-homogeneity to develop which can influence the turbulent flame front propagation and pollutant formation (in particular unburned hydrocarbons and particulate matter) in the optical access window

- An increased opportunity for end gas autoignition and the development of ‘hot-spots’

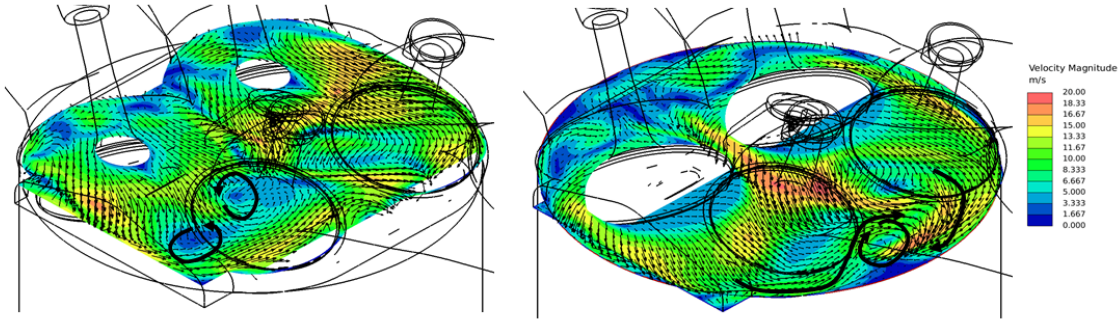

(a) (b)

Figure 9 – CFD model predicted flow fields at 150°ATDC, along two swirl planes intersecting the optical access window, with black arrows indicating rotating vortices and asymmetry generated as a consequence of the optical access window

5. Summary

An engine model was developed using the CFD code STAR-CD for the purpose of modelling the in-cylinder flow field through the intake and compression strokes.

Comparison of the model against experimental indicating data showed the model to predict global in-cylinder quantities well and provided high confidence in the adequacy of boundary conditions supplied to the model. A comparison of the model against intake runner velocities and intake runner flow momentum showed good agreement with experimental data and provided confidence in the models ability to predict the flow field in the intake system across the engine cycle. This also provided confidence in the initial conditions used for the model predictions and that the computational domain had been extended sufficiently far upstream to accurately capture the intake system wave dynamics.

A detailed comparison of predicted and experimental data of the intake valve jet showed the model to be adequate at predicting the valve jet structure. It was identified that the model predicts the intake valve jet to detach from the cylinder head earlier in the cycle than seen in experiment. This is expected to cause a subsequent reduction in effective flow area and potentially be the cause of over predicted valve jet and in-cylinder flow field velocities through the intake stroke. Recirculation zones and valve jet angle are well predicted considering the high levels of cyclic-variability and strong shear characteristics of this flow feature. A comparison between predicted and experimental velocity fields along the bore centreline in the tumble plane showed that whilst in-cylinder velocities appear over predicted early in the intake stroke, the model correctly predicts the general flow structures.

The model was then used to investigate the in-cylinder flow structures occurring within the intake and compression strokes. A highly transient recirculation zone was identified along the nearside cylinder wall and due to its timing within the cycle, could be a source of fuel absorption into the liner oil film for very early fuel injection strategies. The influence of solid boundaries on in-cylinder flow structures was also investigated. Finally, the impact of the optical access window on in-cylinder flow structures was examined. It was found to introduce flow asymmetry between the front and rear of the

combustion chamber and additional recirculation zones in the corners of the pent-roof window. The implications for experimentalists using optical research engines with pen-roof access windows were discussed and recommendations for further improvements were made.

6. Acknowledgements

The authors would like to thank Jaguar Land Rover for supplying the original CAD model and continued financial and technical support, as well as the Engineering and Physical Sciences Research Council (EPSRC) for financial support under grant EP/K014102/1.

7. References

[1] N. Ozdor, M. Dulger, E. Sher:
Cyclic Variability in Spark Ignition Engines A Literature Survey, SAE Technical Paper Series No. 940987, 1994

[2] T. Justham, S. Jarvis, C. P. Garner, G. K. Hargrave, A. Clarke:
Single Cylinder Motored SI IC Engine Intake Runner Flow Measurement Using Time Resolved Digital Particle Image Velocimetry, SAE Technical Paper Series No. 2006-01-1043, 2006

[3] S. Jarvis, T. Justham, A. Clarke, C. P. Garner, G. K. Hargrave, D. Richardson:
Motored SI IC Engine In-Cylinder Flow Field Measurement Using Time Resolved Digital PIV for Characterisation of Cyclic Variation, SAE Technical Paper Series No. 2006-01-1044, 2006

[4] V. Yakhot, S. A. Orszag:
Renormalization group analysis of turbulence. I. Basic theory, Journal of Scientific Computing Vol. 1, No. 1, 1986, 3-51

[5] V. Yakhot, S. A. Orszag, S. Thangam, T. B. Gatski, C. G. Speziale:
Development of turbulence models for shear flows by a double expansion technique, Physics of Fluids A: Fluid Dynamics Vol. 4, No. 7, 1992, 1510

[6] W. Rodi:
Influence of buoyancy and rotation on equations for the turbulent length scale, Proc. 2nd Symposium on Turbulent Shear Flows, 1979, 10.37-10.42

[7] T. Justham:
Cyclic Variation in the Flow Field Behaviour within a Direct Injection Spark Ignition Engine: A High Speed Digital Particle Image Velocimetry Study, Loughborough University, PhD Thesis, 2010

[8] T. Justham, S. Jarvis:
EPSRC Research Report - Combustion Concepts for Sustainable Premium Vehicles - Loughborough Research Report Year 3, 2006